EFFECT OF OFF-NORMAL LOADING ON THE BOND STRENGTH MEASUREMENT OF BONDED REPAIRS

Mildred Lee *, Eudora Yeo **, Madabhushi Janardhana *, C. H. Wang***
***School of Aerospace, Mechanical and Manufacturing Engineering, RMIT University, Australia**
**** Defence Science and Technology Organisation, Australia**
***** Aircraft Structural Integrity - Directorate General Technical Airworthiness (ASI-DGTA), RAAF, Australia**
mildred.lee@student.rmit.edu.au

Keywords: *Bond strength, surface treatment, off-normal loading*

Abstract

Due to surface curvature of aircraft structures, off-normal loading can occur during in-situ bond strength testing using the portable Pneumatic Adhesion Tensile Testing Instrument (PATTI). The aim of this research was to assess, through a combined experimental and numerical investigation, the effects of loading angle and surface treatment on the dry strength of adhesively bonded joints.

1 Introduction

Despite bonded repairs being superior to mechanically fastened repairs in many ways, they are not certified for use on aircraft primary structures when the residual strength of the unrepaired structure falls below the design limit load. The main reason for this conservative approach is that there is no technique to detect a potential drop in bond strength caused by environmental degradation. As a result, repairs to the Royal Australian Air Force and US Air Force aircraft are severely restricted [1, 2].

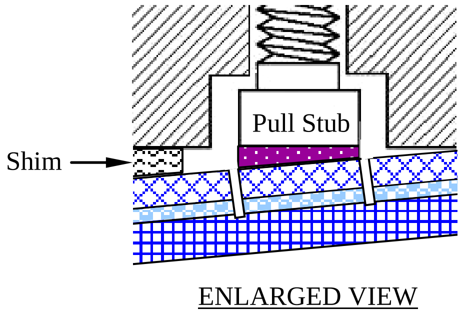

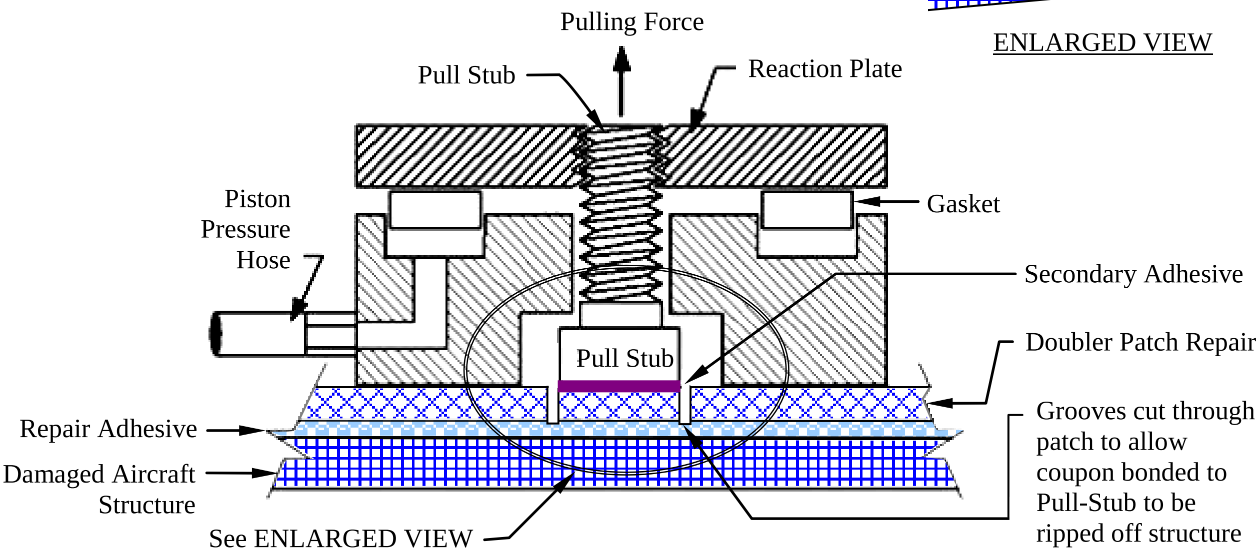

Fig. 1 Configuration of the PATTI test used by DSTO to obtain the residual flatwise tensile strength of bonded repairs on retired aircraft structures. Enlarged view shows typical off-normal loading configuration encountered (and shimmed) when performing PATTI test on curved surfaces.

This study is aimed at characterising the bond durability as represented by both weak and strong bonds. It can be seen that a best initial estimation of a good bond (durability) would help in a robust certification of bonded repairs for primary structures.

In an effort to assess the durability of adhesive bonded repairs, the Defence Science and Technology Organisation (DSTO) has undertaken projects that are sponsored by the Royal Australian Air Force (RAAF) in order to determine the residual strength of bonded patch repairs on retired aircraft parts with the Pneumatic Adhesion Tensile Testing Instrument (PATTI) as shown in Fig. 1.

Originally designed to test the adhesion of coating systems on metal substrates [3], the PATTI test gives an indicative measure of the flatwise tensile strength of the bond, but not the shear strength that governs the effectiveness of the repair. The ability to relate the measured flatwise tensile strength of the bonded repair to the shear strength would enable the determination of the residual strength of the bonded repairs. The tensile and shear strength of structural adhesives, provided failure is cohesive, are generally related via the von Mises criterion or the modified von Mises criterion [4]. Cohesive failure is defined as fracture that occurs within the adhesive layer.

PATTI tests performed on a bonded composite patch repair on a fatigue-cracked F-111C wing [2] generated predominantly cohesion failure with the strength at the edges of the patch being lower than those in the central region. Of particular interest is the fact that the cohesive failure strength varied widely, indicating that the adhesive could have undergone varying degrees of degradation. In addition, some mixed cohesive and interfacial failures observed along the patch edges exhibited generally lower strength compared to the average strength of cohesive failure. These low bond strength results were attributed to a number of factors, including off-normal loading and the tapered edge of the repair patch [2].

This paper presents an experimental investigation to assess the effects of off-normal loading and surface treatment on the dry (no hot-wet conditioning) adhesive bond strength. Scarf joints of varying bonding angles were employed to simulate the off-normal loading of PATTI tests. Finite Element (FE) models were developed to characterise the normal and shear stresses in joints of different angles. The numerical results were employed to assess the ability of the modified von Mises yield criterion to correlate the experimental results.

2 Experimental Method

Tensile butt joints were used to represent the PATTI test configuration used on doubler repairs of retired aircraft parts as shown in Fig. 1. By varying the angle of the scarf joints, different combinations of shear and peel stresses can be tested in addition to representing off-normal loading conditions. Aluminium alloy of 6060 T5 grade bars and 16 x 16 mm sections were lathed to 12.00 mm diameter sections.

Fig. 2: Tensile butt-joints with 0°, 15°, 30°, 60° and 75° bonding angles (from left to right)

The circular cross-sectional areas were then milled to create scarf angles of 15°, 30°, 60°

and 75°, as shown in Fig. 2; single lap-shear (SLS) joints were used to represent 90° loading condition.

A standard surface treatment method employed by the RAAF [5] for adhesive bonding was used as the reference standard for achieving high quality, environmentally durable joints. Two other surface preparation methods,

Table 1: Procedure for the RAAF surface preparation of the bonding area of joints and two other modified versions designed to induce interfacial failure.

Surface Preparation	Procedure
1 (RAAF)	Scotchbrite™ Methyl Ethyl Ketone (MEK), Scotchbrite™ water, Alumina grit blast, Silane
2	Scotchbrite™ MEK, Scotchbrite™ water, Alumina paper abrade, Silane
3	MEK wipe, Water wipe, Alumina paper abrade

as listed in Table 1, were also used to prepare the joints to establish the sensitivity of the shear-tensile relationship to surface preparation techniques.

All joints were bonded with Cytec FM® 300 adhesive film at 177°C for 90 minutes. All bonded joints were tensile loaded to failure in the 50 kN Instron tensile machine at the rate of 1 mm / minute.

3 Relevance of this study for certification of bonded repairs

The studies undertaken in this work are aimed at developing a series of parametric tools to investigate and consequently, if determined to be suitable; complement the use of bonded test coupons as a non-destructive technique to assess the integrity of the load bearing adhesive bonds [6]. Although the joints in this paper were loaded to failure, the ultimate goal of this technique is to ascertain that the bond of the test coupon is able to withstand a minimum applied load which is significantly higher than normal operational loads yet lower than the theoretical ultimate strength of the bond. Whilst PATTI type tests may be considered as an indirect method for characterizing the shear strength of the adhesive bond, alternative methods such as torsion proof-testing of traveler coupon [7] may provide a more direct technique for non-destructive testing of bond strength. It is planned to continue this study with a view to transfer this parametric tool to the RAAF for future management and certification of bonded repairs.

4 Results

Due to the presence of the scrim cloth within the FM®300 adhesive, some cohesive failures occurred that involved the tearing of the scrim cloth. Since the tearing of the scrim cloth occurs within the adhesive and its presence does not contribute any mechanical strength to the bond, this form of failure was treated as cohesive failure in the current analysis. It was observed that increasing the bonding angles from 0° to 30° resulted in a minor decrease in joint strength as shown in Fig. 3.

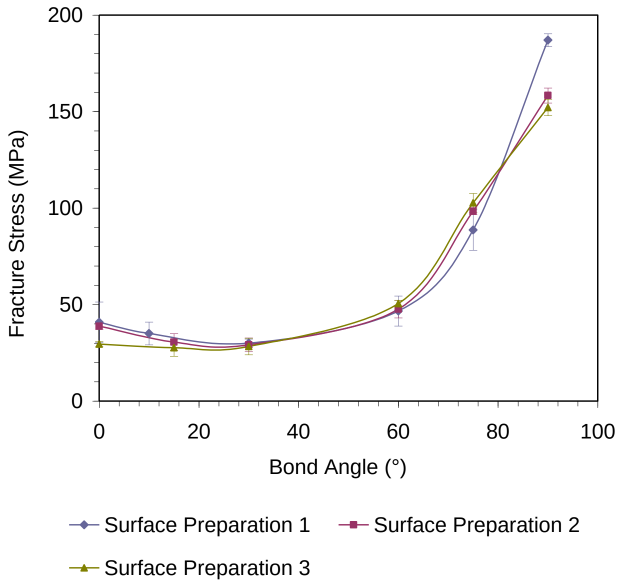

Fig. 3: Joint Fracture Stress versus Bonding Angles for all surface preparation techniques with error bars showing the coefficient of variations.

The fracture surfaces of all the joints generally showed a large number of voids within the adhesive as portrayed in Fig. 4. Due to the scrim failure on some of the fracture surfaces of the 75° and SLS joints, it was not possible to quantify the percentage area voids on those fracture surfaces.

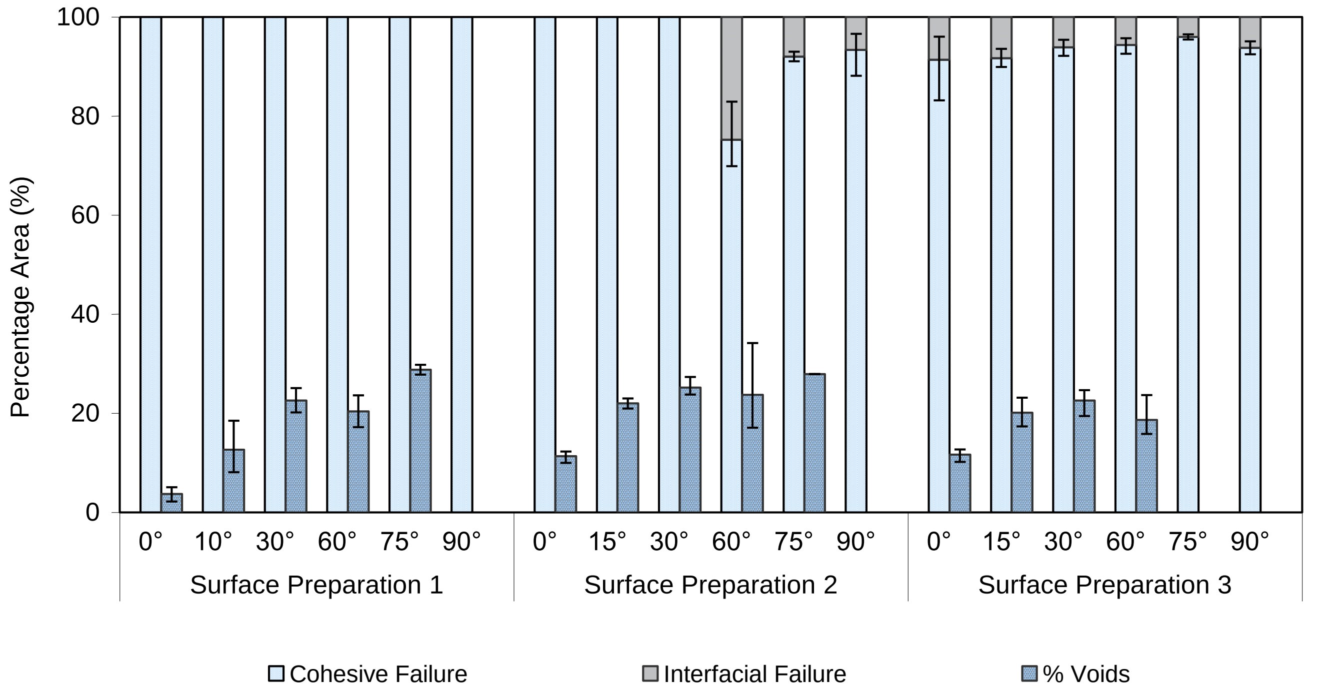

Fig. 4: Percentage of cohesive and interfacial failure observed on fracture surfaces of joints and percentage voids observed on cohesive fracture surfaces. Error bar shows maximum and minimum percentage of area.

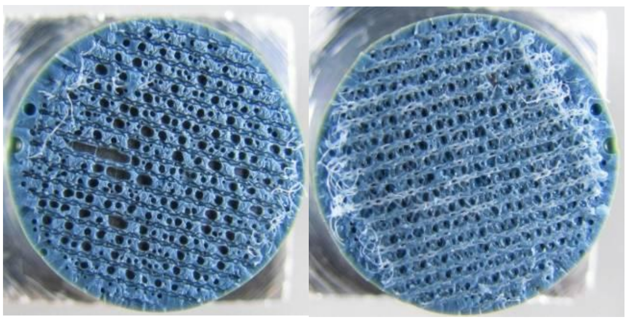

(a)

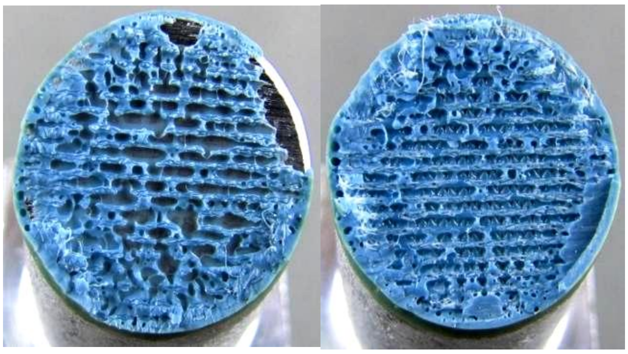

(b)

Fig. 5: Fracture surfaces showing (a) cohesion failure of 0° joint with surface preparation method 2 (b) mixed cohesion-interfacial failure of 30° joint with surface preparation method 3.

The joints with 0° up to 30° bond angles prepared by surface preparation methods 1 and 2 failed in a cohesive mode as shown in Fig. 5a. However, joints prepared by surface preparation method 3 showed mixed cohesive-interfacial failure, with up to a maximum of 9% of fracture surface area being interfacial, as shown in Fig. 5b.

Only one of the 60° joints prepared by surface preparation method 1 showed mixed cohesive-interfacial failure while the rest of the 60°, 75° and 90° joints failed by cohesive failure as shown in Fig. 6a. The joints prepared by surface preparation methods 2 and 3 showed mixed mode fracture as shown in Fig. 6b. Within the cohesive failure region of the 60° joints with surface preparation method 2, large voids were also observed at the interface.

Nonetheless, comparison of the fracture stresses across all three types of surface preparation technique showed that the coefficient of variation is only 5.8% for the 60° joints and 8.4% for the 75° joints, indicating the fracture stresses for the individual joints angle are still considered reliable even if there is no obvious correlation between size of adhesion failure area or void area to fracture stress or the surface preparation techniques.

The fracture stresses of the 90° joints with surface preparation methods 2 and 3 are approximately 17% lower than that of the surface preparation method 1 joints as seen on Fig. 3. It is not known if the area of interfacial failure up to 7% or the total bonded area (due to minor manufacturing differences) had any influence on the reduction of fracture stress.

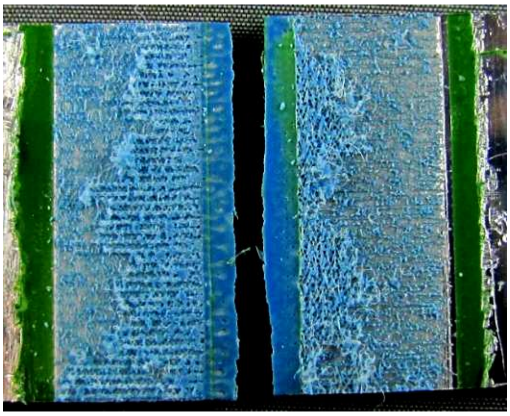

(a)

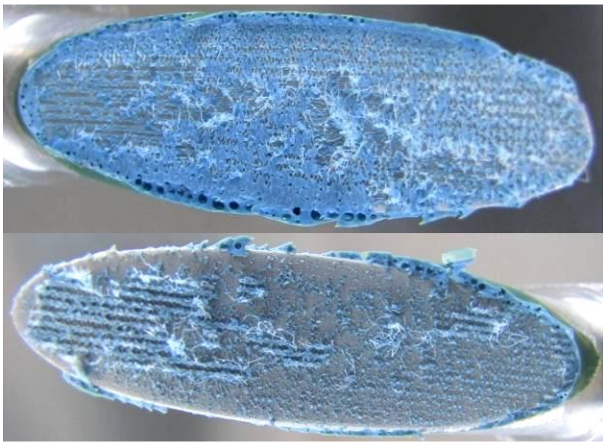

(b)

Fig. 6: Fracture surfaces showing scrim tearing within (a) cohesion failure of a 90° (SLS) joint with Surface Preparation 3 (b) mixed cohesion-adhesion failure of a 75° joint with Surface Preparation 2.

5 Discussion

5.1 Modified von Mises Yield Criterion

The Modified von Mises Yield Criterion is normally used for cohesive failure of adhesives. However, it is not known if it is applicable for correlating the fracture strength when mixed cohesive-interfacial failures occur. To address this question, the experimental results were employed to assess the yield criterion, which relates the deviatoric (von Mises) stress σ_{vm} to the hydrostatic stress component, σ_m via Equation 1:

$$\sigma_{vm} + \alpha\sigma_m = \sqrt{3}\tau_0 \tag{1}$$

whereby τ_0 is the shear yield stress (in pure shear) and α is a material property. σ_{vm} and σ_m are calculated using the principal stresses, $\sigma_1, \sigma_2, \sigma_3$ according to Equations 2 and 3 respectively:

$$\sigma_{vm} = \sqrt{\frac{(\sigma_1 - \sigma_2)^2 + (\sigma_2 - \sigma_3)^2 + (\sigma_3 - \sigma_1)^2}{2}} \tag{2}$$

$$\sigma_m = \frac{\sigma_1 + \sigma_2 + \sigma_3}{3} \tag{3}$$

The σ_{vm} and σ_m were obtained directly from the FE models of the experimental joints. An analytical solution is also provided in the next section to show the calculation method utilized in the linear static analysis FE method.

When σ_{vm} is plotted against σ_m, it can be seen that Equation 1 attempts to describe the relationship between the equivalent deviatoric component of the adhesive to its hydrostatic component as a linear correlation. Mathematically, $\sqrt{3}\tau_0$ becomes the intercept of the σ_{vm} axis, as it was established as the equivalent von Mises yield stress under pure shear and theoretically occurs when the hydrostatic component is zero. This then leaves α as the slope of the curve.

The FM®300 adhesive is considered to obey the yield criterion when it can be shown that the ratio of deviatoric to hydrostatic components within the adhesive affecting its failure varies linearly with the scarf angles 1. If the yielding of the FM®300 adhesive can be described by the Modified von Mises Yield Criterion, then the effect of loading angle in the PATTI tests can be taken into account in analyzing the PATTI results.

5.2 Analytical Analysis

The von Mises and hydrostatic stress components are calculated for an infinitesimal block of adhesive within the bonded joint by assuming the coordinate and stress system shown Fig. 7. The applied stress, σ_{app} is resolved into the normal, σ_n and shear stress components, τ_n acting on the adhesive along the coordinate axes according to Equation 4 and 5.

$$\sigma_n = \sigma_{app}\cos^2\theta \tag{4}$$

$$\tau_n = \frac{1}{2}\sigma_{app}\sin 2\theta \tag{5}$$

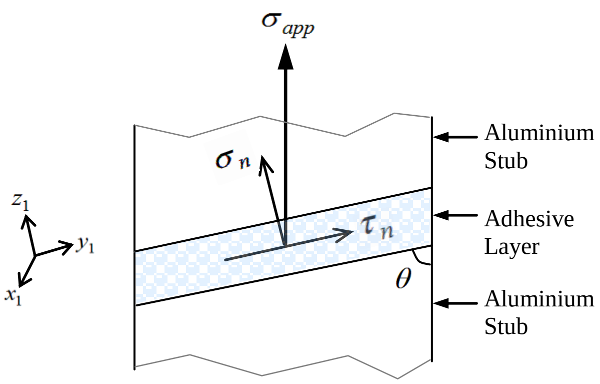

Fig. 7: Orientation of stress vectors within the adhesive layer of the bonded joints.

For the system above, the following components are assumed to be zero, due to the lateral constrain imparted by the stiff Aluminium stubs:

$$\varepsilon_{x_1} = \varepsilon_{y_1} = 0 \tag{6}$$

$$\tau_{xz} = \tau_{yz} = 0 \tag{7}$$

Since the adhesive is an isotropic material, the other normal stress components can be expressed in terms of the normal stress given in Equation 4 using Hooke's Law as follows:

$$\sigma_{z_1} = \sigma_n\ , \quad \sigma_{x_1} = \sigma_{y_1} = \frac{\nu}{1-\nu}\sigma_n \tag{8}$$

Substitution of the stress terms from Equations (5), (7) and (8) into the expressions for the von Mises stress and the hydrostatic stress yield:

$$\sigma_{vm} = \sigma_{app}\times\sqrt{\left(\frac{2\nu-1}{1-\nu}\right)^2\cos^4\theta + \frac{3}{4}\sin^2 2\theta} \tag{9}$$

$$\sigma_m = \sigma_{app}\times\frac{1}{3}\left[\frac{1+\nu}{1-\nu}\right]\cos^2\theta \tag{10}$$

It can be seen that the normalised von Mises stress and hydrostatic stress, σ_{vm}^N and σ_m^N with respect to the applied stress, σ_{app} depend on the loading angle and the Poisson's ratio of the adhesive. These normalised stress values for various loading angles are given in Table 3 for comparison with the values obtained by the FE method described below.

5.3 Finite Element Analysis

Finite Element models of the experimental joints were built in MSC.Patran™ to obtain the stress components within the adhesive layer to verify the applicability of the Modified von Mises Yield Criterion to describe the yielding behaviour of the FM®300 adhesive. In the initial assessment, linear static analyses were performed with MSC.Nastran™.

The stress distributions within the three-dimensional (3D) FE models of the experimental joints were validated against the stress distribution of the axis-symmetric two-dimensional (2D) butt-joint models of Adams et al. [8] and good correlations were found between them. There was only one discrepancy where the shear stress at the peripheral edge of the interface for the 2D model was higher than the 3D model. This same observation was also observed by Alwar and Nagaraja [9].

Nevertheless, 3D models such as the typical model shown in Fig. 8 were considered more suitable for the analyses since a 2D model does not represent a radial slice of the joint configuration as the bond surface of the joint becomes elliptical with increasing bond angle.

The material properties used for the FE analyses are given in Table 2.

Table 2: Material properties used for the FE models from typical published values [10, 11].

Material	Young's Modulus (MPa)	Poisson's Ratio
Aluminium alloy	69000	0.33
FM®300	2280	0.36

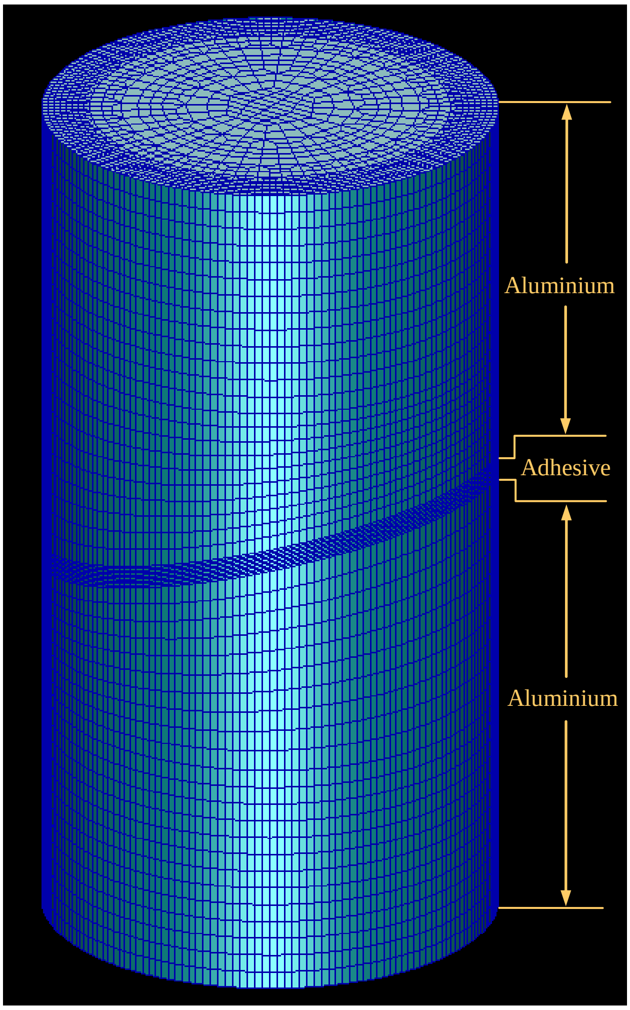

Fig. 8: Finite element model of a 15 angle joint.

The boundary conditions were set to impose constraints on the FE joints in a manner that mimicked the conditions of the actual experimental joints when loaded in the 50kN Instron tensile machine, ie. constraints were applied to the nodes on the lower circular face of the Aluminium section and a unit uniform pressure load was applied to the upper circular face of the Aluminium section.

The relevant stress components required to verify Equation 1 were taken from the mid-layer of the adhesive in the FE models. The overall stress distributions were then averaged and taken as the characteristic stresses affecting the yielding of the adhesive. The normalised von Mises stress ($\sigma_{vm}^{N} = \sigma_{vm} / \sigma_{app}$) and the normalised hydrostatic stress ($\sigma_{m}^{N} = \sigma_{m} / \sigma_{app}$) for each joint are given in Table 3. σ_{app} is the applied stress to produce the von Mises and Hydrostatic components.

Table 3: Normalised von Mises and Hydrostatic stress components within the mid-layer of the adhesive for FE joints with bonding angles corresponding to those used in the experiments.

Bond Angles (°)	Normalised von Mises Stress $\sigma_{vm} / \sigma_{app}$		Normalised Hydrostatic Stress $\sigma_{m} / \sigma_{app}$	
	FE	Analytical Calc.	FE	Analytical Calc.
0	0.5069	0.4292	0.6102	0.7139
10	0.5624	0.5109	0.5970	0.6924
15	0.6388	0.5898	0.5673	0.6661
30	0.8329	0.8162	0.4824	0.5354
60	0.7458	0.7576	0.1887	0.1785
75	0.4254	0.4340	0.0622	0.0478
90 (SLS)	0.2834		0.0202	

As anticipated, when the bond angle of the joints increases, the ratio of normalised von Mises to the normalised Hydrostatic component increases, signifying that the adhesive within the joints experiences a greater shearing effect. The analytical solution in Section 5.2 showed a similar trend as those obtained through these FE analyses; indicating that the analytical solution, which assumes uniform stress distribution in the entire adhesive layer offers a similar level of accuracy as the FE method.

5.4 Correlation of Experimental Data

The normalised von Mises and Hydrostatic components given in Table 3 were multiplied with the failure loads to give the equivalent stress components at the time of fracture. The results are presented in Fig. 9. Linear regression curves were then fitted through the data points pertinent to the joints of a given surface preparation method.

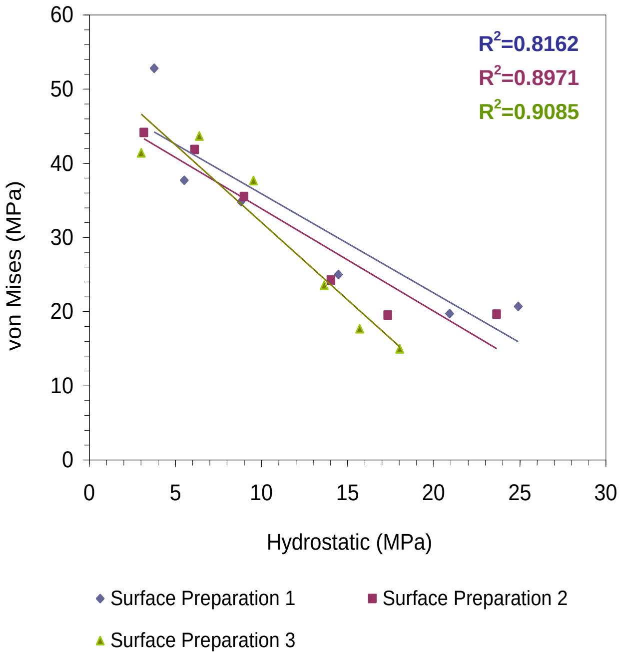

Fig. 9: von Mises equivalent stress component versus Hydrostatic equivalent stress component for all three different surface preparation techniques.

It was suspected that the varying level of voids in the joint might have affected the fracture stresses. To remove this factor, the effective fracture stresses were calculated based on the net cross-sectional area (subtracting the voided area). The 'net' strength values are better fitted with the linear regression curves with greater R-squared values for surface preparation methods 1 and 2 as shown in Fig. 10.

However it should be noted that the fracture stress of joints with partial interfacial failure could not be 'corrected' in this manner because the interfacial bonds might withstand an unknown level of load. If the areas with interfacial failure were assumed to carry zero load, the net cross-sectional area could be further reduced (by subtracting both interfacial area and voided area). The resulting effective fracture stresses are plotted in Fig. 11. It can be seen that the R-square values for surface preparation methods 2 and 3 are much less than

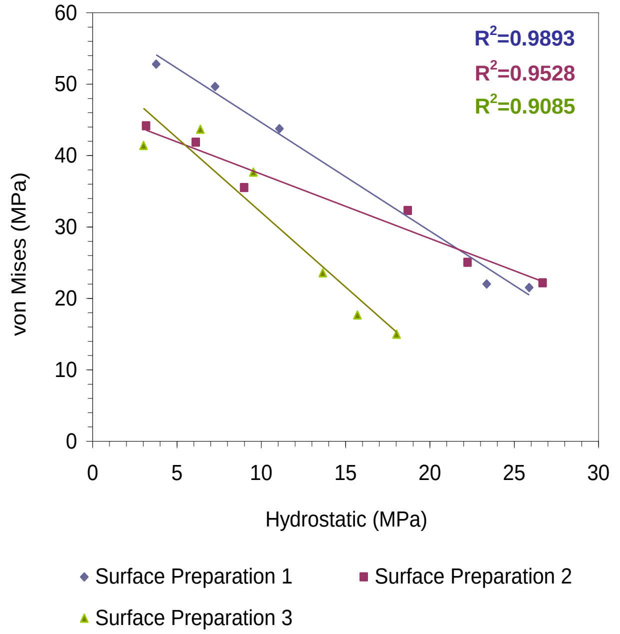

$$\sigma_{vm} = -1.4453\sigma_m + 56.748$$
$$\sigma_{vm} = -0.9872\sigma_m + 46.639$$
$$\sigma_{vm} = -2.0885\sigma_m + 52.917$$

Fig. 10: von Mises equivalent stress component versus Hydrostatic equivalent stress component for all three different surface preparation techniques using the 'corrected' failure stress in the absence of voids.

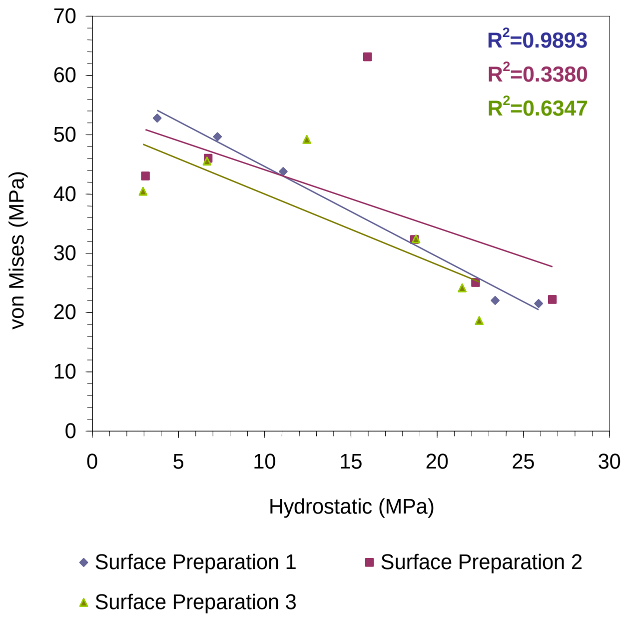

Fig. 11: von Mises equivalent stress component versus Hydrostatic equivalent stress component using the 'corrected' failure stress in the absence of voids and interfacial failure.

unity, indicating that this assumption over predicts the fracture stresses in the absence of interfacial failure. Therefore, regions that showed interfacial failure did carry certain load at the point of fracture.

The slopes of the linear curves show the sensitivity of the adhesive within the joints to Hydrostatic stresses whereby the steeper the slope, the more sensitive it is. Nonetheless, the fact that the data plots could be adequately described by linear relationships for all three different surface preparation techniques shows that the Modified von Mises Yield Criterion can indeed describe the yielding behaviour of the FM®300 adhesive despite the variety of fracture surfaces observed.

5.5 Effects of Off-Normal Loading Angles

Since the modified von Mises criterion can describe the yielding behaviour of the FM®300 adhesive for cohesion failure and mixed mode failure up to 24% interfacial area as shown in Fig. 4, the shear strength of a joint could be inferred from the flatwise tensile strength by multiplying it with the normalized equivalent yield stress under pure shear component via Equation 11:

$$\sigma_{app} = \frac{\sqrt{3}\tau_0}{\sigma_{vm}^N + \alpha\sigma_m^N} \tag{11}$$

The values of σ_{vm}^N and σ_m^N vary with loading angle according to the ratios given in Table 3. In reality, it is unlikely that the PATTI test stubs would ever be loaded at off-normal angles beyond 30° from normal. The material property α, defined as the behaviour of the adhesive under the influence of the three surface preparation methods, is given in Table 4.

Table 4: Material property, α according to surface preparation method as determined from experiments.

Surface Preparation	Material Property, α
1	1.45
2	0.99
3	2.09

Using the values in Table 3 and Table 4, the shear yield strength of the adhesive can be estimated from the off-normal PATTI tests using the following expression:

$$\tau_0 = \frac{(\sigma_{vm}^N + \alpha\sigma_m^N)\sigma_{app}}{\sqrt{3}} \tag{12}$$

The shear yield strengths of the adhesive plotted against the off-normal loading angles in Fig. 11 are almost constant for each surface preparation method; suggesting that this technique removes the influence of the off-normal loading angles on the fracture strength (flatwise tensile strength) to give the inherent shear yield strength of the adhesive. Therefore Equation 12 provides a tool for determining the shear strength of the adhesive bond using the PATTI tests. The effects of the off-normal loading are captured by computational stress analyses. It is important to identify this effect so that the reduced fracture strength of any PATTI stubs bonded / loaded off-normal are not mistaken as a reduction in the inherent adhesive bond strength due to environmental exposure.

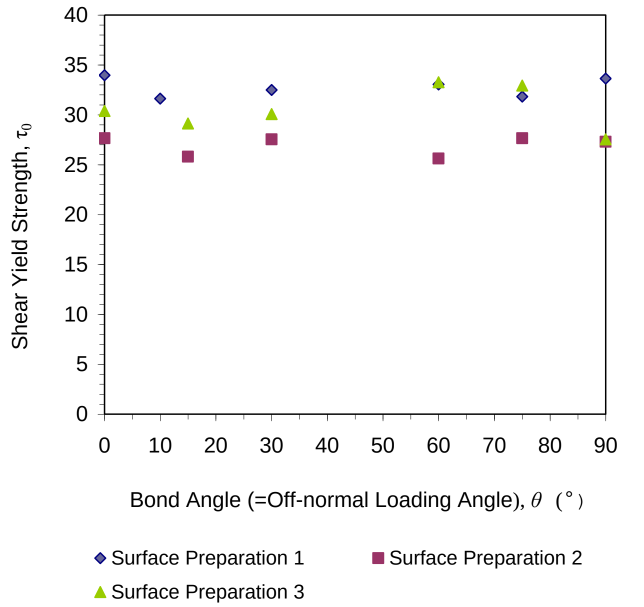

Fig. 11: Shear yield strength values calculated from Equation 12 versus off-normal loading angle

6 Conclusion

The following conclusions summarise the findings from bonded stubs under dry conditions:

- The cohesive failure strengths of joints with FM®300 adhesive can be adequately described by the modified von Mises yield criterion.
- Mixed mode failure (cohesive and interfacial) up to 24% interfacial failure has been found to increase the effect of Hydrostatic stress on the yielding behaviour of FM®300 adhesive.
- Increasing the off-normal loading angle (joint bond angle) in the PATTI test lowers the fracture load.

A method has been presented to estimate the bond shear strength from PATTI tests that accounts for the effect of off-normal loading. The surface treatment methods considered have been found to have negligible effect on the joint strength under dry condition since comparable results were produced.

6 Acknowledgements

The authors gratefully acknowledge the funding from DGTA and the technical support from DSTO (Mark Fitzgerald and Jack Singhavong) and the technical staffs of RMIT University (Patrick Wilkins, Peter Tkatchyk, Bob Ryan and Don Savvides).

7 References

[1] A.A. Baker, A proposed approach for certification of bonded composite repairs to flight-critical airframe structure, *Applied Composite Materials*, Vol. 18, Iss. 4, pp 337-369, 2010.

[2] A. Baker, Structural health monitoring of a bonded composite patch repair on a fatigue-cracked F-111C wing, *DSTO-RR-0335*, 2008.

[3] ASTM, Annual book of astm standards, in: ASTM D4541 - 09e1 Standard Test Method for Pull-Off Strength of Coatings Using Portable Adhesion Testers, ASTM, 2010.

[4] C.H. Wang, P. Chalkley, Plastic yielding of a film adhesive under multiaxial stresses, *International Journal of Adhesion and Adhesives*, Vol. 20, pp 155 - 164, 2000.

[5] A.N. Rider, Surface treatments for field level bonded repairs to aluminium and titanium structure, Air Vehicles Division, Defence Science and Technology Organisation, DSTO-TR-2153, 2008

[6] G.P. McBroom, Method of forming and indirect testing of a bond of or in an aircraft component, in: United States Patent, Airbus Operations Limited, Bristol (GB), United States, 2010.

[7] A. Baker, D. Bitton, J. Wang, Development of a proof test for through-life monitoring of bond integrity in adhesively bonded repairs to aircraft structure, *International Journal of Adhesion and Adhesives*, Vol. 36, pp 65-76 2012.

[8] R.D. Adams, J. Coppendale, N.A. Peppiatt, Stress analysis of axisymmetric butt joints loaded in torsion and tension, *Journal of Strain Analysis for Engineering Design*, Vol. 13, No. 1, pp 1-10, 1978.

[9] R.S. Alwar, Y.R. Nagaraja, Elastic analysis of adhesive butt joints, *Journal of Adhesion*, Vol. 7, No. 4, pp 279-287, 1976.

[10] C.C. Lee, A. Crosky, D. Kelly, Determination of the mechanical properties of adhesives for use in design of bonded joints in composite structures, in: ICCM-10, Whistler, B.C., Canada, 1995, pp. 511-518.

[11] K.M. Liechti, T. Freda, On the use of laminated beams for the determination of pure and mixed-mode fracture properties of structural adhesives, *The Journal of Adhesion*, Vol. 28, No. pp 145-169, 1989.

Copyright Statement